



# Separation of full, empty, and partial adeno-associated virus capsids via anion-exchange chromatography with continuous recycling and accumulation

Yong Suk Lee<sup>a</sup>, Jaeweon Lee<sup>b</sup>, Kun Fang<sup>c</sup>, Gretchen V. Gee<sup>c</sup>, Benjamin Rogers<sup>c</sup>, David McNally<sup>b,c</sup>, Seongkyu Yoon<sup>b,\*</sup>

<sup>a</sup> Department of Pharmaceutical Sciences, University of Massachusetts Lowell, Lowell, MA 01854, USA

<sup>b</sup> Department of Chemical Engineering, University of Massachusetts Lowell, Lowell, MA 01854, USA

<sup>c</sup> MassBiologics, University of Massachusetts Chan Medical School, Mattapan, MA 02126, USA

## ARTICLE INFO

### Keywords:

Gene therapy  
Adeno-associated virus  
Continuous anion-exchange chromatography  
N-Rich  
Full/empty ratio  
Partial capsid

## ABSTRACT

The field of recombinant adeno-associated virus (rAAV) gene therapy has attracted increasing attention over decades. Within the ongoing challenges of rAAV manufacturing, the co-production of impurities, such as empty and partial capsids containing no or truncated transgenes, poses a significant challenge. Due to their potential impact on drug efficacy and clinical safety, it is imperative to conduct comprehensive monitoring and characterization of these impurities prior to the release of the final gene therapy product. Nevertheless, existing analytical techniques encounter notable limitations, encompassing low throughput, long turnaround times, high sample consumption, and/or complicated data analysis. Chromatography-based analytical methods are recognized for their current Good Manufacturing Practice (cGMP) alignment, high repeatability, reproducibility, low limit of detection, and rapid turnaround times. Despite these advantages, current anion exchange high pressure liquid chromatography (AEX-HPLC) methods struggle with baseline separation of partial capsids from full and empty capsids, resulting in inaccurate full-to-empty capsid ratio, as partial capsids are obscured within peaks corresponding to empty and full capsids. In this study, we present a unique analytical AEX method designed to characterize not only empty and full capsids but also partial capsids. This method utilizes continuous N-Rich chromatography with recycling between two identical AEX columns for the accumulation and isolation of partial capsids. The development process is comprehensively discussed, covering the preparation of reference materials representing full (rAAV-LacZ), partial (rAAV-GFP), and empty (rAAV-empty) capsids, N-rich method development, fraction analysis, determination of fluorescence response factors between capsid variants, and validation through comparison with other comparative techniques.

## 1. Introduction

Since the first recombinant adeno-associated virus (rAAV) clinical trial in 1990s, rAAV has emerged as one of the primary viral vectors used for gene therapy to treat various rare genetic diseases [1,2]. Based on its low immunogenicity, low pathogenicity, and a broad range of therapeutic applications and target tissues dependent on different serotypes [3–5], several rAAV-based gene therapy products (Glybera, Luxturna, Zolgensma, Elevidys, Hemgenix, Roctavian, and Upstaza) have been approved by Food and Drug Administration (FDA) or European Medicines Agency (EMA) and many more are currently in clinical trials

[6–11]. rAAV is also one of the most extensively researched and characterized vectors due to their favorable safety profile, efficacy in gene delivery, and versatility in targeting different tissues. Most commonly, transient transfection of Human embryonic kidney 293 (HEK293) cells using three different plasmids including transgene flanked by Inverted Terminal Repeats (ITRs) on both ends, *Rep* & *Cap*, and helper plasmids to manufacture non-enveloped rAAV vectors [12]. This involves the formation of serotype-specific capsid made up of viral proteins (VP) 1/2/3 in 1:1:10 ratio, which are translated from *cap* gene, with aids from Rep40/52/68/78 encoded in *rep* gene and some accessory proteins including assembly-activating protein (AAP) and membrane-associated

\* Corresponding author at: 1 University Ave, Lowell, MA 01854, USA.

E-mail address: [seongkyu.yoon@uml.edu](mailto:seongkyu.yoon@uml.edu) (S. Yoon).

<https://doi.org/10.1016/j.jchromb.2024.124206>

Received 4 April 2024; Received in revised form 28 May 2024; Accepted 11 June 2024

Available online 15 June 2024

1570-0232/© 2024 Elsevier B.V. All rights reserved, including those for text and data mining, AI training, and similar technologies.

accessory protein (MAAP) for replication and packaging the single-stranded gene of interest (GOI) into the capsid [13,14].

Due to lack of a complete understanding and controls in the manufacturing process, not all capsids successfully encapsidate the desired genome and there are inevitable populations of empty (no transgene), partial (truncated transgene), and other (host cell DNA or residual plasmids) capsids as product impurities as described in Fig. 1 [15]. Research indicates that there is high variability in full (F) and empty (E) capsid ratio depending on different critical attributes in the transient transfection process leading to high batch-to-batch variability [16–18]. This capsid heterogeneity poses not only burdens to downstream process but jeopardizes quality controls as co-existence of capsid impurities in the final gene therapy product creates significant impacts on dosing determination, efficacy, and safety. The presence of capsid impurities is known to reduce transduction efficacy, induce particle aggregation, and produce undesired human innate and adaptive immune responses leading to the development of Anti-AAV antibodies [19–25]. Partial (P) and other capsids containing non-target genes that include truncated GOI, residual plasmids or host cell DNA pose greater safety concerns because they may deliver uncharacterized genes with genotoxicity and/or immunotoxicity, especially if the early region 1 (E1) sequence in HEK293 is mispackaged [26,27]. Empty capsids are reported to behave as a decoy and therapeutic capsid escape from AAV clearance by neutralizing antibodies [28]. However, regardless of the magnitude of the impact on efficacy and safety, the capsid ratio in the final gene therapy product must be accurately reported.

Similarities shared between full capsids and empty/partial capsids make it difficult to separate and accurately report full/empty (F/E) ratio [16,29]. Capsids, structured with VP1, VP2, and VP3 viral proteins in 1:1:10 ratio, are ~ 25 nm in diameter regardless of the presence of single-stranded DNA (ssDNA) up to 4.8 kb in size inside the capsid [30]. There is a slight difference in isoelectric point (pI) and density due to the presence of negatively charged ssDNA inside the capsids [31,32]. Many different analytical techniques have been reported to characterize full and empty capsid ratios based on these differences. These include A260/A280 ultraviolet (UV) absorbance (Abs), size exclusion chromatography coupled to multiangle light scattering (SEC-MALS), analytical ultracentrifugation (AUC), transmission electron microscopy (TEM), cryo-electron microscopy (cryo-EM), charge detection mass spectrometry (CDMS), two-dimensional liquid chromatography mass spectrometry (2D-LC-MS), qPCR&ELISA combination, and Anion-exchange column chromatography (AEX) [33–39]. The key issues with current analytical methods are that (1) well-established common methods often do not fully satisfy the needs for high throughput, short turnaround, and sufficient specificity, (2) newer methods lack enough validation and justification for their use, and (3) standardized protocols are not established and reproducibility between laboratories is poor [38]. Moreover, each method exhibits clear pros and cons [38]. Both industry and regulatory agencies still need a robust, sensitive, reproducible, and sample-sparing

method that allows complete quantification of full (F), partial (P), and empty (E) and characterization of capsid quality.

HPLC is an acknowledged technique for its repeatability, high-throughput capacity, and compatibility with Good Manufacturing Practice (GMP) quality control (QC) standards [40]. Among other chromatography-based techniques, ion-exchange chromatography (IEX) facilitates the separation of empty and full capsids based on subtle distinctions in their surface charges attributed by the presence of vector genome. Compared to cation exchange chromatography (CEX), AEX is reported to show better resolution at milder elution conditions with more optimized protocols and established base knowledge [33,40–43]. The slightly higher isoelectric point (pI) of empty capsids (~6.3) compared to that of full capsids (~5.9) results in their earlier elution compared to DNA-containing capsids during shallow linear gradient elution with an increase in salt concentration [44]. Certain studies indicate that the dipole moments of the capsid are considered low, questioning the influence of ssDNA on the capsid protein's surface charge [45]. The phenomenon, while not fully elucidated, has prompted multiple AEX methods successfully developed for both preparative separation and analytical purposes [33,40,43,46–48]. Despite extensive efforts to optimize capsid separation, one of the main limitations with AEX as an analytical method is the lack of isolation of partial capsids – a heterogeneous population of capsid partially-filled with a spectrum of DNA sizes [26,49]. Partially filled capsids exhibit similar structural and physicochemical properties to full capsids and often remain obscured within the empty peak, the full peak or overlapping portions, potentially leading to an overestimation of full capsids. This poses challenges in downstream purification and polishing for achieving higher purity and accurate characterization of the full, partial, and empty capsid profile in gene therapy products [13]. Despite efforts to optimize AEX methods, research has highlighted the ineffectiveness of improving baseline separation of partial capsids from full and empty capsids, with variables such as column types (e.g., monolith or non-porous beads), housing materials (e.g., stainless steel or PEEK), buffer content (e.g., BTP, AMPD, AMPSO, CHES or CAPSO), and salt types (e.g., NaCl, KCl, or TMAC) showing minimal impact on resolution [50]. Fluorescence detector (FLR) measures the native fluorescence of aromatic amino acids (tryptophan, tyrosine, and phenylalanine) in the capsid protein, as discussed in various research about their accuracy and sensitivity over ultraviolet detector (UVD) at 260 nm/280 nm in F/E ratio measurement [33,40,47,48]. In contrast, the UV signal at 280 nm is often elevated due to the contributions from both protein and DNA, diminishing its relative sensitivity, especially empty capsid detection in scarce amounts [33,40,48]. High sensitivity is required especially for analysis of analytes, which are in low concentration.

N-Rich continuous chromatography, utilizing twin columns with recycling between them, ensures effective enrichment and purity of target compounds from complex mixtures [51,52]. Primarily employed in preparative chromatography, N-Rich overcomes the trade-off

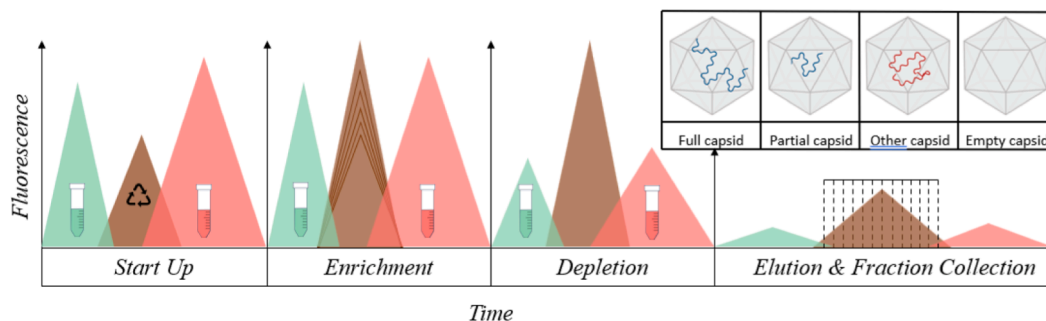


**Fig. 1. N-Rich rationale and analytical application.** Simplified representation of different types of capsids produced during rAAV production. Full capsid containing intact therapeutic transgene; Partial capsid containing truncated transgene; Other capsid containing host cell DNA or residual plasmids; Empty capsid containing no transgene. The bottom schematic representation describes N-Rich application for rAAV F/P/E ratio analytical method development that is operated via four major steps: (1) start up, (2) enrichment, (3) depletion, and (4) elution and fraction collection.

between productivity and purity often associated with traditional chromatography by recycling a portion containing the desired product and impurity, thereby possibly enhancing the chances of separation [53–55]. The N-Rich process, specifically designed to accumulate target compounds, can be applied to develop a chromatography-based analytical tool to separate not only full and empty capsids, but also provide insights on partial capsids within the sample. In contrast to the typical N-Rich rationale focused on enriching a target molecule amid impurities, the new analytical method requires collecting and quantifying all peaks corresponding to capsids with different transgene sizes (F, P, or E) to determine a complete F/P/E ratio. Partial capsids, which are typically difficult to identify due to a broad range of DNA size and lack of insight into the exact sequence, are treated as a target molecule that is being accumulated via multiple cycles of recycling, while empty and full capsids, which elute at different retention times (Rt) during AEX, are separately collected. In the initial “start-up” step, equilibration and initial loading of a sample mixed with full, partial, and empty capsids (Fig. 1). Weakly binding capsids, specifically empty capsids under anion exchange settings, elute first and are collected. After recycling the mixed portion, the more strongly binding full capsids elute last and are collected separately. The second enrichment step involves multiple cycles of continuous chromatography using twin columns for accumulation of partial capsids in the overlapping portion. Within a predetermined recycling window, the mixed portion is fed into the second column, which is simultaneously regenerated prior to sample feeding through in-line dilution, along with the new feed, a fresh sample injection. The new feed is identical to the feed injected to the first column in concentration, but not in volume (to be discussed in Section 3.4.2). This results in a progressive accumulation and concentration increase of the target molecule with each cycle. The third step, depletion, includes the final chromatography run without adding a new feed to improve the final target purity before the last elution. During the elution and fractionation step, the separated target material is eluted with a shallow gradient over twin columns connected in series to maximize resolution. The eluted material is collected using a fraction collector and quantified separately [51,52]. The research works highlighted in this paper confirm if partially filled capsids elute out at intermediate retention time in between those of empty and full capsids and often are obscured in a peak corresponding to full capsids and if the baseline separation can be enhanced by re-introducing the mixed portion multiple times to the column providing additional opportunities for separation. The newly developed N-Rich method demonstrated successful enhancement in F/P/E ratio using FLRs; however, a few limitations related to the detectors were noted, necessitating additional experiments. Since automated recycling window selection based on FLRs is not supported by the current software, manual recycling window selection was performed based on Rt from the preliminary batch run prior to the N-rich run. Additionally, fluorescence calibration is required based on the determined response factors (RF) for different transgene sizes.

## 2. Materials and methods

### 2.1. Chemical and reagents

Bis-tris propane (BTP,  $\geq 99.0\%$ ), tetramethylammonium chloride (TMAC, reagent grade,  $\geq 98\%$ ), magnesium chloride ( $\text{MgCl}_2$ , anhydrous,  $\geq 98\%$ ), and ethanol (pure, 190 proof) were purchased from Sigma-Aldrich, and sodium hydroxide (NaOH, Extra Pure,  $\geq 99\%$ ) and Pluronic™ F-68 non-ionic surfactant (10x) were purchased from Thermo Fisher Scientific. Sodium chloride (NaCl,  $\geq 99.5\%$ ) and sodium acetate (NaOAc,  $\geq 99\%$ , extra pure) were purchased from Honeywell Research Chemicals and VWR, respectively. The buffers were prepared by dissolving appropriate chemicals in LC-MS-grade water purchased from J.T.Baker, and pH was adjusted using 6 mol/L hydrochloric acid (HCl, Millipore Sigma).

### 2.2. Reference samples used for the method development

Three distinct rAAV2 reference materials, rAAV2-LacZ, rAAV2-GFP, and rAAV2-Empty, were sourced from Virovek (Hayward, CA), and MassBiologics (Fall River, MA). These materials served as the basis for developing the analytical method outlined in Table 1. rAAV2 containing LacZ (4,676 bp) gene was treated as a full capsid containing the intact desired genome due to its larger size. Similarly, rAAV2-GFP reference material, containing a smaller genome of 2,434 bp, was considered as a pseudo-partial capsid, reflecting an intermediate transgene size that include truncated transgene, host cell DNA and residual plasmid DNAs. Virovek rAAVs were produced in Sf9 cells by infection with rBV-inCap2-K2R-inRep-kozak-hr2 and rBV-CMV-LacZ, rBV-CMV-GFP or none, followed by two rounds of cesium Chloride (CsCl) gradient ultracentrifugation. CsCl was removed via buffer exchange using 2 PD-10 desalting columns, and the final samples were stored in a solution containing 1xPBS, 0.001 % pluronic F-68, and 100 mM sodium citrate. rAAV2 samples obtained from MassBiologics were produced via transient transfection of HEK293 cells. Purification was initially performed through capture affinity chromatography (1 mL Capto AVB column / equilibration: 20 mM sodium phosphate, pH 7.2, 350 mM NaCl, wash 1: 20 mM sodium citrate pH 6.0, 1 M NaCl, wash 2: 20 mM sodium citrate pH 6.0, 350 mM NaCl, and elution: 50 mM sodium citrate pH 3.0, 350 mM NaCl), followed by ultracentrifugation. Final samples were stored in a solution composed of 80 mM sodium chloride, 10 mM sodium phosphate, and 0.001 % Poloxamer 188 at a pH of 7.3. Depending on the specific analytical methods used, the samples were either undiluted or diluted at various rates to achieve the optimal concentrations using the recommended diluents. The aliquoted reference materials were stored at  $-80^\circ\text{C}$  to prevent multiple freeze-thaw cycles, minimizing sample degradation.

### 2.3. Quantitative polymerase chain reaction (qPCR) for single-target vector genome titer measurement

The samples were treated with DNase I in DNase Reaction Buffer (New England Biolabs, USA) and incubated for 1 h at  $37^\circ\text{C}$ , following the manufacturer's instructions. Subsequently, proteinase K (New England Biolabs, USA) was added to the sample, followed by 1 h incubation at  $55^\circ\text{C}$  and 10 min inactivation step at  $95^\circ\text{C}$ . Each sample was subsequently diluted 125-fold in water through serial dilution (5, 25, and 125-fold). In preparation for quantification of unknown samples, six dilutions of rAAV5 standard material (MassBiologics, USA) were prepared using the same method employed for the rAAV2 samples for use as a standard curve. Each plate included negative controls (no primer/probe mixture), no template controls (NTCs), and positive controls (pAAV-CMV-GFP linearized with HindIII or (pAAV-CMV-LacZ-bGH linearized with BspQI). qPCR analysis targeted the transgenes, either or both eGFP and/or lacZ using a PrimeTime qPCR probe assay (Integrated DNA Technologies, USA) depending on the targets in the sample. Primer/probe sequences are listed in Table 1. Each 20  $\mu\text{L}$  qPCR reaction consisted of 10.0  $\mu\text{L}$  TaqMan™ Universal PCR Master Mix (ThermoFisher Scientific, USA), 1.0  $\mu\text{L}$  primer/probe mix (500 nM primers/250 nM probe), 6.0  $\mu\text{L}$  molecular biology grade water, and 3.0  $\mu\text{L}$  125-fold diluted sample. The reactions were executed on a CFX96 Real-Time PCR Detection system (Bio-Rad, USA). The thermal cycle involved an initial step of 20 sec at  $95^\circ\text{C}$ , followed by 39 cycles of two-step thermal cycling of 3 sec at  $95^\circ\text{C}$  and 30 sec at  $60^\circ\text{C}$  with a plate read. Data analysis was conducted in Microsoft Excel. Regression analysis for plots of the  $\log_{10}$  rAAV5-eGFP standard concentration versus the associated quantification cycle (Cq) was performed to generate the standard curve. The derived equations were then utilized to determine the Genome copies (GC) titer.

**Table 1**  
Reference materials transgene and primer/probe sequence information.

Reference material	Use	transgene size	Primer sequence (5'-3')	Probe Sequence (5'-3')
rAAV-LacZ	Pseudo-full capsid	4,676 bp	Forward: GAACCGCATCGAGCTGAA Reverse: TGCTTGTCGGCCATGATATAG	/56-FAM/ATCGACTTC /ZEN/AAGGAGGACGGCAAC/3IABkFQ/
rAAV2-GFP	Pseudo-partial capsid	2,434 bp	Forward: GCC GAA ATC CCG AAT CTC TAT C Reverse: AGC AGC AGC AGA CCA TTT	/56-FAM/ATT GAA GCA /ZEN/GAA GCC TGC GAT GTC /3IABkFQ/
rAAV2-Empty	Empty capsid	0 bp	N/A	N/A

#### 2.4. Enzyme-linked immunosorbent assay (ELISA) for capsid particle titer quantification

Capsid protein (CP) titers were measured using a Progen AAV2 titration ELISA kit 2.0R (Progen Biotechnik GMBH, Germany) per the manufacturer's instructions. rAAV2 samples were serially diluted from 25 ~ 125-fold to achieve the final concentration within the Progen AAV2 empty capsid standard curve range between  $3.91 \times 10^7$ – $2.50 \times 10^9$  capsids/mL. The plate setting included serially diluted empty capsid standards included with the kit, unknown samples, and blanks in duplicate. The optical density (OD) was measured with a Synergy<sup>TM</sup> LX Multi-Mode microplate reader (BioTek, USA) at 450 and 650 nm. The background OD values at 650 nm were subtracted from the 450 nm measurements to perform for all samples and standards. The rAAV2 CP titer of unknown samples was calculated in Microsoft Excel using the four-parameter logistic (4-PL) standard curve generated from the serially diluted kit controls.

#### 2.5. F/E ratio measurement with analytical AEX

The analytical AEX method employed 1.66 mL (4.6 mm x 100 mm) protein-Pak Hi Res Q column (Waters, USA) with quaternary ammonium ligand and an Agilent 1100 HPLC system with G1321A FLR. Other columns including BIA separation CIMac AAV E/F analytical column and YMC BioPro QA-F were also evaluated, but not included in the final batch chromatogram design due to challenging column regeneration or backpressure higher than acceptable pressure limit of Contichrom preparative chromatography system with two FLRs (~20 bar). The column was equilibrated with the equilibration buffer containing 20–70 mM BTP, 2 mM MgCl<sub>2</sub>, and 0.1 % of Pluronic F-68 buffer at pH 9. 0.1 % v/v Pluronic buffer was used to prevent rAAV sample aggregation and unwanted binding to the plastic in the chromatography systems [56]. Each sample was diluted in the equilibration buffer such that the final injection load is  $1 \times 10^{10}$  ~  $1 \times 10^{11}$  CP and a total injection volume of less than 3 % of the column volume (CV) was used. The column was washed with 4 CV of the equilibration buffer, followed by full and empty capsid elution from the column by applying either step (data not shown) or linear gradient. The elution buffer contained the same constituents as the equilibration buffer, but different types of salts, Tetramethylammonium chloride, Sodium Chloride, or sodium Acetate were added. The entire steps were performed at 0.4 mL/min and monitored under UVDs (260&280 nm) and FLR (excitation: 280 nm, emission: 348 nm).

#### 2.6. TEM F/E ratio measurement

Transmission Electron Microscopy measurement was conducted in UMass Chan Medical School. Glow discharge treatment was performed on carbon-coated TEM grids using Pelco easiglow (Ted Pella, USA) for increased hydrophilicity and enhanced adhesion of rAAV2 on the grids. 3–4  $\mu$ L of sample diluted to meet the target concentration of around  $1$ – $2 \times 10^{12}$  GC/mL. After 30 sec of incubation, the sample was slowly absorbed using water-soaked filter paper to remove unbound residuals from the grid. Upon 1 min incubation after the treatment of 8 drops of 1 % Uranyl Acetate for negative staining, the excessive uranyl acetate was removed using filter paper. Six to ten images were collected at  $43,000 \times$  and  $135,000 \times$  times magnification using Philips CM10 (Philips, Japan).

Empty capsids with a dark spot in the center due to the negative staining and full capsids with a relatively lighter center were manually counted and assigned either full or empty. The total number of full capsids divided by the total number of rAAV2 particles in the image provided the ratios, which were averaged to determine the percentages.

#### 2.7. Batch chromatogram design

To design a continuous enrichment process, batch design was developed using Contichrom Cube 30 continuous chromatography system (ChromaCon AG, Switzerland). Among other columns tests, A 1 mL HiTrap Capto Q strong anion exchange column was selected for AEX using Contichrom Cube due to high repeatability in terms of Rt (RSD = 0.09 min) and peak size (RSD < 5 %), and acceptable peak symmetry (mean = 1.01). The column equilibrated with equilibration buffer (20 mM BTP, 2 mM MgCl<sub>2</sub>, 0.1 % Pluronic buffer, pH9.0) for 5 CV. Subsequently, 500  $\mu$ L of  $1 \times 10^{10}$  ~  $1 \times 10^{11}$  CP reference materials (either individual or mixed) was loaded using system pump, followed by 5 CV post-wash with equilibration buffer. The sample was separated by slow 30 CV linear gradient using elution buffer (20 mM BTP, 2 mM MgCl<sub>2</sub>, 250 mM NaOAc, 0.1 % Pluronic buffer, pH 9.0). The entire steps were performed at 0.5 ml/min and monitored via FLR (excitation: 280 nm, emission: 348 nm) except strip and cleaning steps where flow rate of 1 ml/min was used. The column was cleaned and stripped using 2 M NaCl (5 CV) and 1 M NaOH (5 CV) and regenerated with equilibration buffer (15 CV). The batch design was used as a reference to create continuous enrichment process. For further information, fractions collected from the batch process was pooled and analyzed using ELISA and qPCR to evaluate elution profile of different reference materials and to determine the most optimum portion of the chromatogram to recycle in the new analytical method.

#### 2.8. N-Rich (enrichment) process for F/P/E ratio measurement

Two 1 mL HiTrap Capto Q columns (Cytiva, USA) were employed for continuous chromatography with recycling between the columns. The Contichrom Cube 30, equipped with two RF-20A fluorescence detectors (Shimadzu, Japan) and two TOY18DADH UV detectors (ECOM, Czech Republic), along with Fraction Collector Foxy R1 (Knauer, Germany), were utilized. The continuous N-Rich process, designed to adhere to the same protocol as single-column batch separation, was implemented using N-Rich wizard, a N-Rich design aid included in the ChromIQ software of Contichrom Cube. Recycling windows and collecting windows for each reference material are shown in Fig. 2. Due to lower limit of detection and more consistent results, fluorescent detectors were selected as the main detector to monitor the elution profile of capsid contents. The software determines recycling windows based on either retention time or UV signal changes, not fluorescence signal; therefore, the continuous process had to be conducted based on retention time. A preliminary test batch was conducted prior to the N-Rich method to accurately determine the retention time of each peak, which tends to slightly vary depending on the sample, column, and buffer preparation. Recycling windows from the template method were adjusted based on the retention times determined from the batch test run. The alignment of FLRs located directly after each column outlet was carefully controlled. The N-Rich wizard determined switching time, recycling and collecting

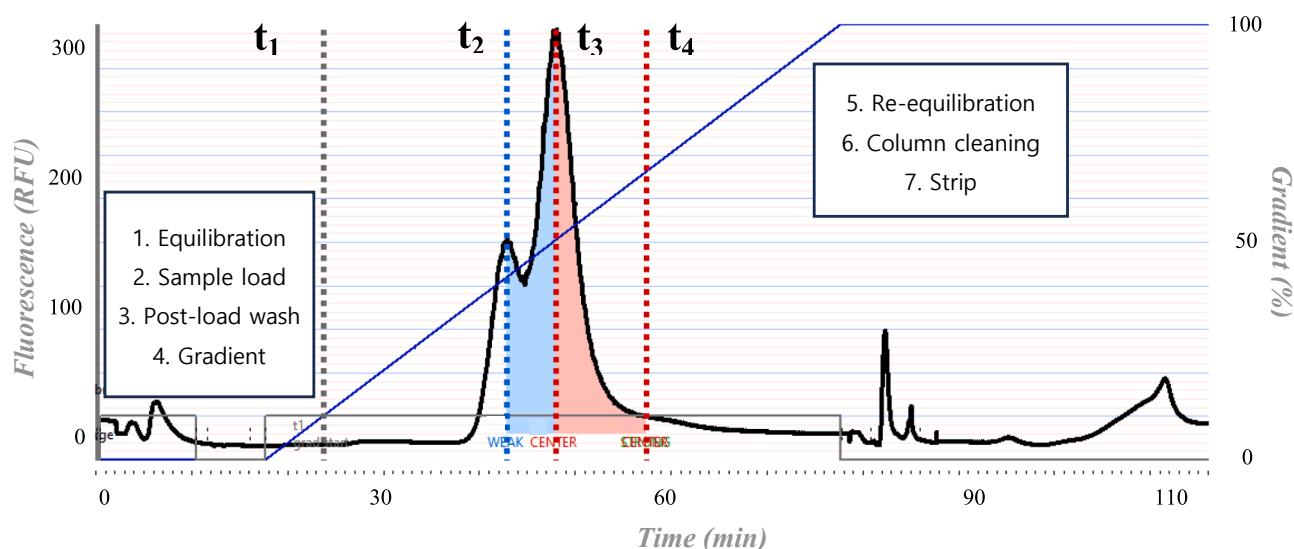


**Fig. 2. N-Rich (enrichment) method design process using software.** This shows how N-Rich method is developed using Chrom IQ software. Initial N-Rich method developed based on the batch chromatography design with sufficient overlapping. Modifications were made to selectively collect the portion mainly concentrated with rAAV-empty (white:t1-t2) was collected from one outlet. The mixed portion predominantly with AAV-GFP (blue:t2-t3) was recycled and fed to the next column with a new feed. Another portion collected the portion containing mostly rAAV-LacZ (red:t3-t4). (For interpretation of the references to color in this figure legend, the reader is referred to the web version of this article.)

windows, inline dilution, and loads based on the 4 section boarders ( $t_1 \sim t_4$ ) assigned. The N-Rich protocol, executed over three cycles (six column switches), was designed to collect pure empty and full capsids while recycling mixed portions with higher partial capsids to the next column for accumulation of partial capsids. The finalized operating method followed the sequences (Startup, Accumulation, Depletion & Elution) described above (Fig. 1) and the final protocol are shown in Table 1.

### 3. Results and discussion

#### 3.1. Rationale and strategy for new analytical method development

Chromatography-based analytical methods offer notable advantages, characterized by high repeatability, reproducibility, and automation, coupled with a relatively low limit of detection (LOD) and rapid turnaround time. The primary challenge in current methods lies in achieving baseline separation of partial capsids. Partial capsids, exhibiting a spectrum of DNA sizes, possess distinct or intermediate charges based on their transgene size. These capsids will tend to elute out at intermediate retention time in between those of empty and full capsids and often obscured in two corresponding peaks. The research is to explore if the baseline separation can be enhanced by re-introducing the mixed portion multiple times to the column providing additional opportunities for separation. In order to conduct the experiment, a N-Rich method utilizing twin anion exchange columns was developed. Incorporating fluorescence detection enhances sensitivity and accuracy by measuring the native fluorescence of aromatic amino acids in the capsid protein. The methodology involves several key steps: (1) development of comparative techniques for comparison (AEX-HPLC, qPCR&ELISA, and TEM), (2) batch method design intentionally exhibiting sufficient overlapping between full and empty capsids, (3) method transfer to the Contichrom Cube, which is capable of running continuous recycle, (4) fraction analysis via qPCR&ELISA to determine the elution profile of each reference material, (5) N-Rich method design, (6) quantification of N-Rich results, and, finally, (7) purity validation of N-Rich eluents.

#### 3.2. Batch chromatogram methods

##### 3.2.1. AEX-HPLC

AEX-HPLC was developed utilizing the protein-Pak Hi Res Q column. Method optimization for consistent full and empty capsid separation involved exploration of various conditions (BIA separation CIMac AAV E/F analytical column, Waters Protein-Pak Hi Res Q, YMC BioPro QA-F, and Cytiva Capto Q), Buffer concentration (20–70 mM BTP), pH (9 and 10), flow rate (0.3–0.8 mL/min), injection load ( $1 \times 10^{10} \sim 3 \times 10^{11}$  CP), salt type (NaCl, NaOAc, and TMAC), gradient type (linear, step, 5 % and 10 % isocratic hold) and Pluronic agent concentrations (0.001 ~ 0.1 %); however, no significant improvement was observed from the explorations, which aligned with Aebischer et al [50]. Key findings related to the finalization of the AEX method are summarized in the supplementary document (Supplementary Figure S1).

##### 3.2.2. AEX batch design using Contichrom Cube 30

Based on the base knowledge obtained during AEX-HPLC method development and optimization, an AEX method was developed using Contichrom Cube 30 for N-Rich execution. To accommodate system and detector pressure limit of 10 bar, 1 ml HiTrap Capto Q anion exchange column was employed. Operation flow rate was selected to mitigate doubled back pressure from two columns in series during the recycling process. Both mobile and elution buffers were prepared with 20 mM BTP at pH 9, as BTP has one of its pKs at 9.1, along with 2 mM  $MgCl_2$  for its reported benefits in resolution and on-column stability [57]. Addition of high concentration  $MgCl_2$  (~18 mM) irreversibly degraded some of the columns tested, so minimal concentration was selected. 250 mM NaOAc was added in the elution buffer to prepare a gradient with adequate ionic and displacement strengths. Unlike protein-Pak Hi Res Q column, TMAC demonstrated inconsistency with the Capto Q column, resulting in pre-elution and varying symmetry factors (S) of 0.7 or 1.8 from the elution peaks from duplicated runs indicating peak fronting and tailing. NaOAc, aligned with application notes, generated repeatable separation both in linear and step gradient elution. 0.1 % Pluronic buffer was added to prevent possible aggregation. Details, including Strip and Cleaning in Place (CIP), are outlined in Table 2. The batch design in Fig. 2 and Supplementary Figure S2 aimed for intentional full and empty capsid overlap, ready for improvement through recycling. Samples, diluted in

**Table 2**

Batch method developed for AEX using Contichrom Cube 30.

Step	Column Volume	Buffer
EQUILIBRATION	5	Buffer A (20 mM Bis-tris Propane, 2 mM MgCl <sub>2</sub> , 0.1 % Pluronic buffer, pH 9.0)
LOAD	0.5	Capto Q, AAV2 sample diluted in Buffer A (sample: 1E + 10 ~ 3E + 11 CP)
POST-LOAD WASH	5	Buffer A
ELUTION	30	Linear gradient, 0 % to 100 % of Buffer B (20 mM Bis-tris Propane, 2 mM MgCl <sub>2</sub> , 250 mM NaOAc, 0.1 % Pluronic buffer, pH 9.0)
STRIP / CIP	5 / 5	2 M NaCl / 1 M NaOH
RE-EQUILIBRATION	15	Buffer A
Column – 1 ml HiTrap Capto Q AEX column (Cytiva)		
Detection – FLR (EX:280 nm, EM:348 nm)		
Flow rate – 0.5 ml/min (mostly), 1 ml/min (strip and CIP)		
Injection volume – 500 µL		

equilibration buffer to achieve an injection load of approximately  $1 \times 10^{11}$  CP, were injected using the system sample pump. An automated purging method was employed, and the sample pump's repeatability was assessed with triplicate F capsid injections, yielding relative standard deviations (RSD) of 0.09 %, 4.7 %, and 4.6 % for retention time, area under the curve, and max peak height, respectively (Supplementary Figure S3). Full to empty capsid ratios were calculated based on peak areas and compared with ELISA data for the mixed F/E sample (Table 3). The AEX-derived F/E ratio, adjusted using a fluorescence RF of 1.68 (to be discussed in section 3.6), was 64.4 %, slightly lower but still comparable to the 70.3 % F/E ratio.

### 3.3. Fraction analysis using qPCR&ELISA combination

Fraction analysis was conducted to analyze elution profiles of each capsid type from the developed AEX method. AEX was performed with a mixed sample (F:  $2.90 \times 10^{11}$  CP, P:  $1.81 \times 10^{11}$  CP, and E:  $4.90 \times 10^{10}$  CP in 500 µL injection), and fractions were collected, as depicted in Fig. 3a. There is a higher probability of identifying partial capsids with intermediate DNA size in the overlapping region between peaks corresponding to empty and full capsids. Fig. 3a illustrates fluorescence signals for two peaks, typically identified as empty and full capsids, while no insights on partial capsids can be obtained as they are embedded in the two peaks. Fraction analysis utilized ELISA for total capsid titer and two sets of qPCR assays for GC titers targeting LacZ and GFP genes (Fig. 3b). The fluorescence signal highly correlated with the total capsid titer from ELISA data. Additionally, fraction #9 and 10 exhibited highly pure empty capsids, as qPCR assays showed “below of limit of detection” results for both LacZ and GFP genes, while ELISA data indicated the presence of rAAV2 capsids in the fractions. It was also observed that the capsid containing GFP gene were predominantly clustered toward the earlier portion of the second peak. The left skewness of offline qPCR analysis on partial capsids (Fig. 3b) suggested that there is an elution profile difference during AEX between capsids depending on transgene sizes in the mixed sample. Moreover, the apex for the two reference materials differed, implying distinct retention times for the two types of capsids when running through an AEX column. The distribution of partial capsids peaked at fraction #13, while the full capsid apex was found in fraction #14. A minor peak in GFP qPCR assay for sample #15 was observed. This possibly indicates the presence of aggregated and/or degraded capsids due to on-column instability,

**Table 3**

Validation of AEX method by comparing with ELISA-based F/E ratio.

Material	Sample preparation (ELISA)				Measurement (AEX)				Response Factor applied (1.69)*	
	Concentration (CP/ml)	Injection Volume (µL)	Injection Load (CP)	Ratio (%)	Rt (min)	Area under Curve (RFU*min)	Ratio (%)	RSD (%)	Adjusted Area (RFU*min)	Ratio (%)
F	$2.32E + 11$	500	$1.16E + 11$	70.3	48.1	1137	75.2	5.1	676.8	64.4
E	$9.79E + 10$	500	$4.90E + 10$	29.7	42.9	374.3	24.8	4.7	374.3	35.6

\*Response Factor (RF) was determined to compensate elevated FL signal for full capsid compared to that of empty capsid.

mitigated even with the presence of divalent cations. Based on the elution profile of different capsid types, the optimum recycling window was determined using two dotted red lines in Fig. 3b, where the highest proportion of partial capsids was observed.

### 3.4. Modified n-rich

#### 3.4.1. Instrument setup and preliminary test batch

To adapt the N-Rich method developed using N-Rich wizard software in accordance with the new analytical application, slight modifications were made to the hardware setup and method. The final setup is illustrated in Fig. 4, providing a detailed explanation of the process in chronological order: (1) the sample was introduced to column C1; (2) the elution of capsids was monitored by FLR1, and the method dictated that (3) empty capsid was collected via designated outlet as they were eluted first. The portion intended for recycling was fed directly via (4) inline dilution to the (5) second column. Simultaneously, full capsid eluted from the C1 after the recycling window was collected separately via an outlet. In the same manner, the (6) elution, (7, 9) collection, and (8, 10) recycle occurred in C2. During elution step, N-Rich method connects two columns in series via internal recycle path, which is used to transfer the recycled portion to the next column during enrichment step, and a final shallow gradient elution is conducted for the overlapping portion from the last step of enrichment. Accumulated partial capsids were collected separately through fraction collection (11). The keys to successful N-Rich methods for this application were accuracy of recycling window, signal calibration and alignments between two FLRs, and column repeatability for sufficient regeneration before the next feed. Along with a regular signal alignment, the method was adjusted to have sufficient column volume for strip, CIP, and re-equilibration steps. To compensate for even small variations among different HiTrap columns prior to the N-Rich run, a preliminary test batch was performed for more accurate determination of the recycling windows. Fig. 5 shows one of the preliminary batch chromatograms used to adjust the recycling windows for the subsequent N-Rich method. It is worth noting that the current N-Rich software lacks the capability to control recycling based on FLR signal changes, but solely on retention time in the absence of UVD as the main detector. Implementing such functionality would significantly streamline future procedures, reducing time and complexity.

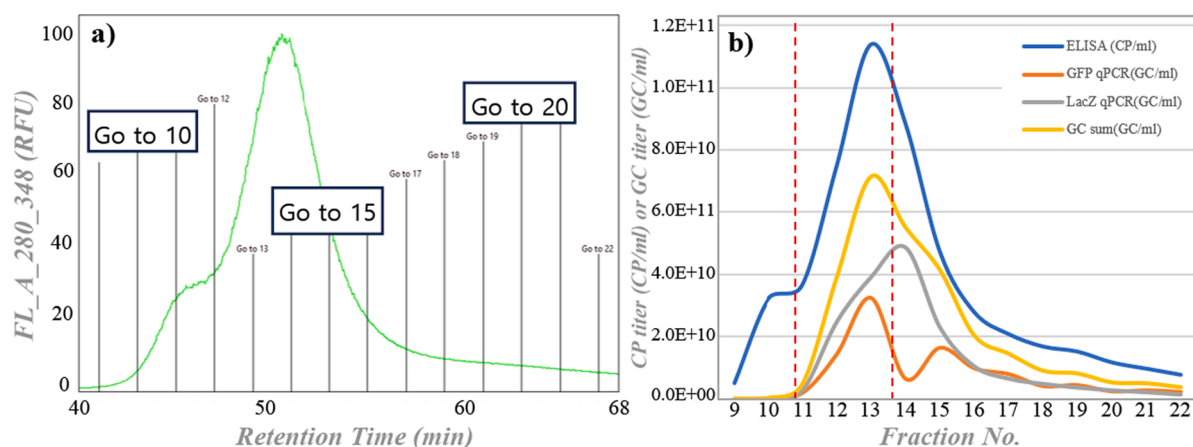


**Fig. 3. Fraction analysis using qPCR&ELISA combination.** (a) fraction collection from AEX batch chromatography monitored by fluorescence detector (Ex: 280 nm and Em: 348 nm) and (b) fraction analysis using qPCR&ELISA assays. Vertical lines in (a) indicates fractions collection command executed by fraction collector. Fraction analysis was performed using ELISA for capsid titer (blue) and qPCR for GC titers targeting both LacZ gene (gray) and GFP (orange) genes. Both GC titers were combined and graphed (yellow) to determine dilution profiles of capsids with transgene. The optimum recycling window is indicated by two dotted red lines where higher ratio of partial capsids is observed compared to empty and full capsids. (For interpretation of the references to color in this figure legend, the reader is referred to the web version of this article.)

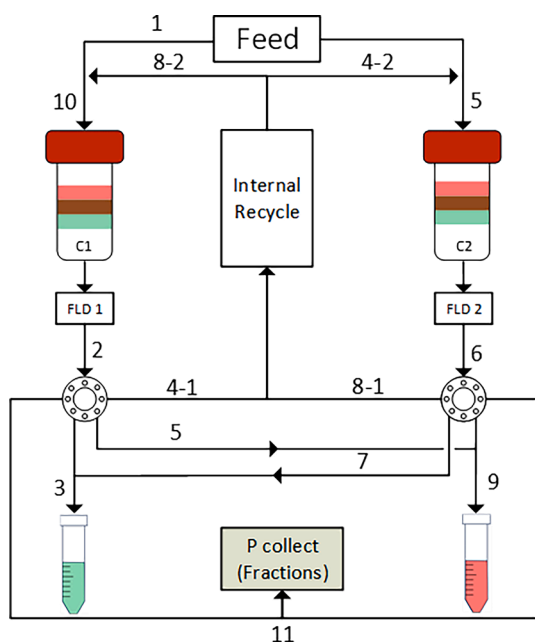


**Fig. 4. Contichrom Cube instrument setup and scheme.** Schematic view of modified N-Rich method for collection of pure E and F and recycle of mixed portion for separation of P. the labels are in chronological order of the process. Simplified representation: Green (Empty capsid), Red (full capsid) Brown (mixed). The recycles between two columns (C1 and C2) and collection of F and E capsids are dictated in automatic and continuous manner. (For interpretation of the references to color in this figure legend, the reader is referred to the web version of this article.)

### 3.4.2. Modified n-rich run

Leveraging insights from the preliminary batch chromatography, the recycling windows were adjusted to selectively recycle the portion containing the highest concentration of partial capsids, while relatively pure empty and full capsids were collected. Three cycles consisting of six separate separations with recycle for accumulation were conducted, followed by final elution of the accumulated overlapping portion from the last separation (Fig. 6). In a continuous process, one column is regenerated and cleaned for the next separation while elution occurs in the other column. The entire enrichment process was depicted in a single

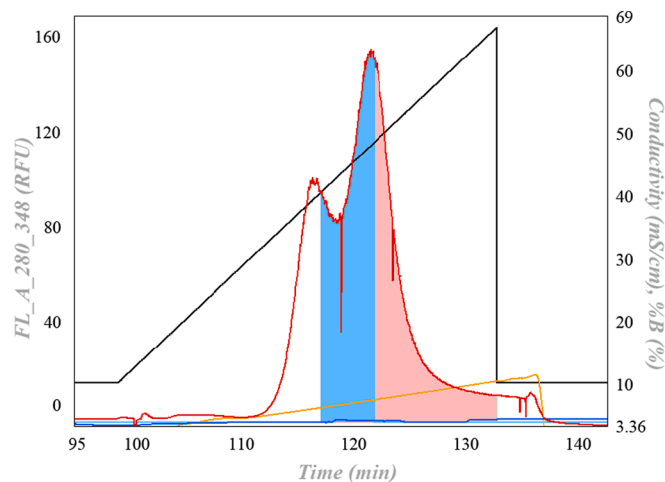


**Fig. 5. Preliminary test batch and determination of recycling window.** The recycling window, represented by blue color, is adjusted based on the fraction analysis in the most conservative manner to include the highest portion of partial capsids. Red line represents the elution of capsids monitored by FLD (Ex:280 nm, Em: 348 nm). Black line represents %B of elution buffer containing 250 mM NaOAc, whereas yellow line represents the conductivity increase aligned with increase in the salt concentration. (For interpretation of the references to color in this figure legend, the reader is referred to the web version of this article.)

plot (Fig. 6a). Ideally, the six chromatograms should be identical in size since identical columns were used three times each with sufficient regeneration and cleaning steps included in each method. The N-Rich run reaches a steady-state characterized by minimal fluctuations in peaks during each switch, where the number of capsids removed in the waste (white and red in Fig. 6a) equaled the number of capsids introduced from the new feed. Excessive addition of capsids in the new feed led to a progressive increase in peak height and total FLR signal, resulting in peak broadening after two cycles (data not shown). To address this, the method was refined to introduce only 417  $\mu\text{L}$  (500  $\mu\text{L}/\text{min} \times 50 \text{ sec}$ ) of feed to the column during each switch, instead of the initial 500  $\mu\text{L}$ . This adjustment enabled three cycles of accumulation without complications, followed by depletion and the final shallow gradient elution step (Fig. 6b). During the final elution, the columns

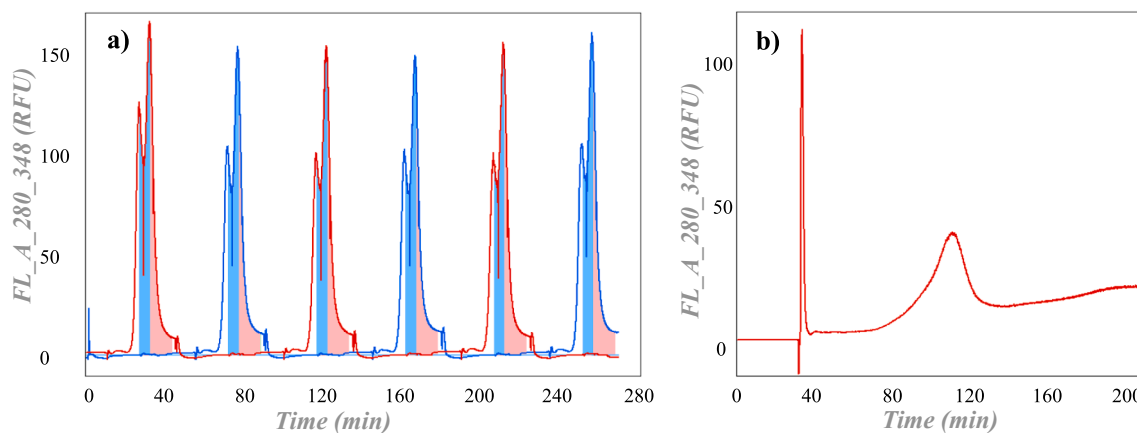


**Fig. 6. Modified N-Rich method run.** (a) Three cycles of N-Rich consisting of six separate separations with two columns are illustrated in a single plot. Red and blue-lined chromatograms correspond to fluorescence signals generated from column 1 and 2, respectively. For continuous process, one column is regenerated and cleaned for the next separation while elution is taking place in the other column. White (empty, collect), Blue (mixed, recycle), Red (full, collect). (b) The final elution was performed using two columns in series (C2 → C1). It illustrates the final elution of accumulated target compound (blue portion from the last elution) in a shallow gradient via two columns connected in series at the end of the recycling cycles. (For interpretation of the references to color in this figure legend, the reader is referred to the web version of this article.)

were connected in series (C2 → C1), and the bed height was doubled. The final elution via shallow gradient is expected to contain a high proportion of partial capsids compared to full and empty capsids. For quantification purposes, the total area under the curves was integrated for each capsid and assessed. The overall runtime of the method was 626 min (startup: 40 min, enrichment: 270 min, depletion: 46 min, and elution: 270 min). The results and chromatograms of the accumulation and elution steps suggest that there is significant room for shortening the method by optimizing the gradient during elution, such as start B% and slope. This optimization could significantly reduce the overall runtime.

### 3.5. Quantification

#### 3.5.1. Standard curve

Using the same column and AEX conditions, a five-point standard curve was generated by injecting five different concentrations of rAAV2-LacZ reference materials. The concentration range was between  $1.95 \times 10^{10} \sim 2.90 \times 10^{11}$  CP/mL, with each standard undergoing  $2 \times$  serial dilution using the mobile buffer. Duplicate injections of 500  $\mu$ L were performed for each standard loaded. Correlation analysis between total fluorescence (FL) signals and concentration, based on the area under the curve, yielded a linearity curve equation:  $y = 6E-09x-7.8227$ , accompanied by an  $R^2$  value of 0.999 (Supplementary Figure S4). Standard deviations for each sample ranged between 2.05 and 11.41, with a tendency for higher RSD at lower injection loads. The lower limit of detection (LOD) was calculated to be approximately  $1.37 \times 10^{10}$  CP/ml, and the limit of quantification (LOQ) was determined to be  $4.16 \times 10^{10}$  CP/ml, ensuring an RSD smaller than 5%. The equations used to calculate LOD (1) and LOQ (2) are shown below. The linear curve equation was employed to quantify peaks with unknown concentrations.

(1) Limit of detection (LOD)

$$LOD = \frac{3.3 * \text{standard error}}{\text{slope of calibration curve}}$$

(2) Limit of quantification (LOQ)

$$LOQ = \frac{10 * \text{standard error}}{\text{slope of calibration curve}}$$

#### 3.5.2. RF and quantification of n-rich data

Theoretically, RF between full and empty capsids is expected to be close to 1 due to the absence of intrinsic fluorescence in DNA, facilitating a direct comparison of fluorescence signals emitted by full and empty

capsids. However, experimental results from various full, partial, and empty capsids demonstrated divergent fluorescence signals, even when an equal number of capsids were separately injected. The normalized signals, adjusted by the number of capsids (spiked-in known capsid titers), were also different among capsids (Table 4). Analyzing triplicate runs of each reference material yielded significant findings. (1) There is a retention time difference between partial (51.9 min) and full (52.3 min) capsids by 24 s, which additionally corroborates the findings determined by the qPCR results in Fig. 6b. (2) The observed discrepancies in normalized fluorescence signals suggests necessitating determination of RFs relative to empty capsids for each full and partial capsid to correct bias. (3) The calculated RF of full capsid (1.68) is higher than that of partial capsid (1.35), indicating that the RF is not only serotype-specific but also dependent on the DNA size inside the capsid. Reported RFs for AAV6.2 (undisclosed transgene) and AAV8 (GFP) were 1.3 and 1.9, respectively [43,58]. The RF and its magnitude difference depending on the transgene size could be due to relatively smaller but still impactful intrinsic fluorescence from DNA and/or slight conformational changes in capsids by interactions between DNA and capsid protein, resulting in changes in hydrophobicity environment [59]. The RFs determined were applied to the batch results (Table 3) and N-Rich data (Table 5). The auto-integration function facilitated obtaining total area under the curves for empty capsids and full capsids from 6 switches. Similarly, the area under the curve for partial capsids was obtained from the final elution chromatogram. Following the application of the RFs, the concentrations for each reference material were calculated using the standard curve and compared with the ELISA capsid titers. The concentration measured by N-Rich AEX showed elevated numbers compared to ELISA. Moreover, the new analytical method revealed an F/P/E ratio of 2.7:1:2.3, deviating from the originally prepared 3:1:2 ratio.

#### 3.5.3. Comparison with other techniques

Finally, the capsid ratio obtained using the new analytical method was compared with that of other techniques, encompassing qPCR&ELISA, TEM, and FL-AEX-HPLC. Samples mixed with all three types of F/P/E capsids in 3:1:2 ratio were prepared and analyzed by different techniques in duplicate. The “actual ratio” in Fig. 7 indicates the intended ratio during sample preparation, which was based on the ELISA capsid titers of reference materials. Notably, qPCR & ELISA, TEM, and FL-AEX-HPLC lacked information on partial capsids due to limited capabilities. In reality, the qPCR genome titer employs specific primers targeting the transgene (only LacZ gene, not LacZ and GFP genes), and

**Table 4**  
Response factor determination.

Sample	Run	Inj. Load (CP)	Rt (min)	STD (min)	AUC (RFU*min)	RSD (%)	AUC/CP (RFU*min/CP)	Response Factor (RF)
E Average	Triplicate	6.17E + 10	45.9	0.05	160.6	5.22	2.60E-09	1
P Average	Triplicate	8.33E + 10	51.9	0.12	298.4	6.12	3.58E-09	1.35
F Average	Triplicate	8.89E + 10	52.3	0.15	386.2	5.22	4.34E-09	1.69

**Table 5**  
Quantification of F/P/E ratio using N-Rich method.

	Assay	F (collected)	P (Recycled)	E (collected)	F Ratio	P ratio	E ratio	Simplified Ratio		
								F	P	E
Average Area under Curve (RFs applied)	New	1493.06	515.76	1260.85	N/A	N/A	N/A	N/A	N/A	N/A
Measured concentration	Calculation	2.50E + 11	8.73E + 10	2.11E + 11	45.54 %	15.93 %	38.52 %	2.7	1.0	2.3
RSD	Calculation	5.39	3.07	3.34	2.14	6.32	0.08	N/A	N/A	N/A
Injected (preparation)	ELISA	1.63E + 11	5.49E + 10	1.07E + 11	50.16 %	16.90 %	32.93 %	3.0	1.0	2.0

Standard curve equation:  $y = 6E-09x - 7.8227$ ,  $R^2 = 0.99$

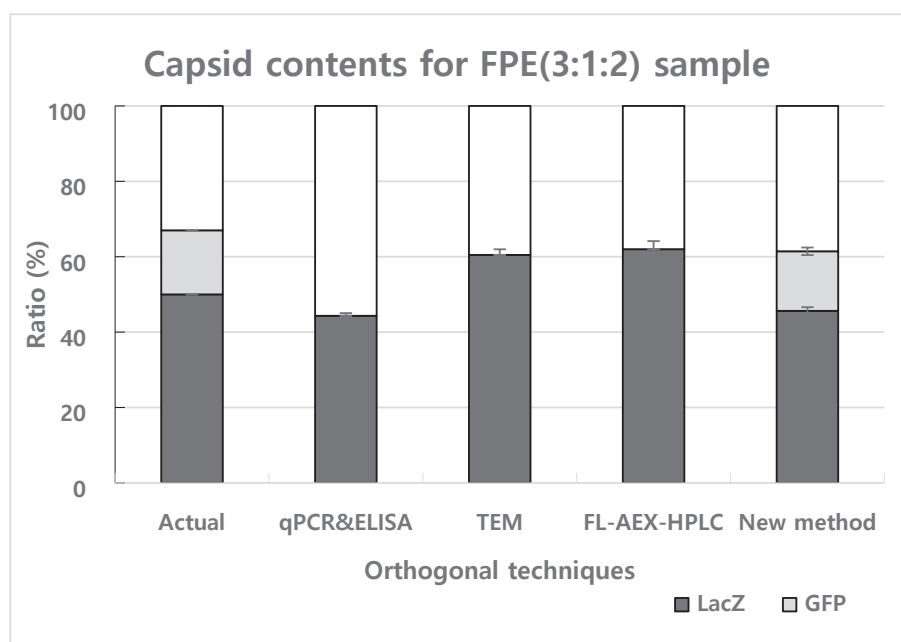


**Fig. 7. F/P/E ratio comparison with comparative techniques.** Capsid ratio obtained from different analytical methods. The “actual” ratio was established through ELISA capsid titer, upon which mixed samples were formulated (F:P:E = 3:1:2). qPCR&ELISA is the ratio of genome and total capsid titer. TEM data was obtained after the negative staining using 1 % uranyl acetate, which was unable to provide clear distinction between full and partial capsids based on the degree of staining. The FL-AEX-HPLC was performed using protein-Pak Hi Res Q column. The new method indicates developed N-Rich AEX method using Contichrom Cube. Error bars were included for all the measurements by different assays. Standard deviation were added to each measurement.

the qPCR&ELISA data in Fig. 7 reflects the current limitations of the assay commonly used by biopharmaceutical industry and academia by including only qPCR data targeting LacZ sequence. Truncated LacZ genes will be factored into the full capsid ratio if the preserved sequence includes the target amplicon; conversely, if the targeted sequence is truncated or entirely missing, it will contribute to the empty capsid ratio, leading to inaccurate quantification and ratio determination. Moreover, both qPCR and ELISA assays, due to their labor-intensive nature and multiple sample preparation steps, such as enzyme treatment, incubation, dilutions, were prone to inconsistent data. TEM-based capsid content determination heavily relied on negative staining with 1 % uranyl acetate. Theoretically, the absence of DNA inside the capsid leads to staining in empty capsid whereas partial and full capsids are not stained due to the filled space. It was difficult to perform the staining consistently throughout the sample on the grid, and the degree of

staining and the contrast was different depending on where on the grid is observed under the microscope. Moreover, low pH (4.5 ~ 4.9) of the uranyl acetate staining solution often caused aggregation of rAAV samples which were prepared in pH 7. The challenges in vivid distinguishment of partial capsids and full capsids under TEM led to an implied inclusion of partial capsids as full capsids. Additionally, the manual counting of each capsid required subjective judgement, particularly when dealing with empty capsids that were not completely stained but showed broken circular staining lines due to shrinkage during staining process (Supplementary Figure S5). However, baseline separation of partial capsids was not achievable, as demonstrated in Fig. 3b, leading to an overestimation of full capsids. Among the comparative techniques compared, the newly developed method demonstrated a close alignment with the anticipated F/P/E ratio of 3:1:3 in spike-in experiments, establishing its superiority in the ratio

determination of three different capsid contents.

### 3.5.4. N-Rich Analysis

N-rich results and samples collected were evaluated using qPCR assays targeting GFP or LacZ genes. Fig. 8 depicts the distribution of each capsid across three final destinations: E collection tube, F collection tube, and P fraction collector. The analysis revealed that during the final elution step of N-Rich, 75.49 % of partial capsids, determined by GFP-targeting qPCR assay, were isolated in the fraction collector, while 19.16 % and 5.35 % co-eluted with F and E capsids, respectively. Furthermore, 84.62 % of F capsids were located in the designated F collection tube, with the remaining found in the fraction collector.

However, the concentration of F capsids found in the E collection tube were below the limit of detection for the qPCR assay, indicating more confident separation between F and E capsids compared to P capsids, which are known to be more challenging to separate due to their physicochemical similarities. Moreover, and impact of transgene on fluorescence signals could possibly have an impact on the peak size and shape and accurate recycling window selection. This clearly demonstrated the necessity of improving the method that includes enhanced recycle window selection, optimized methods, and increased number of recycling cycles.

## 4. Conclusion

The presence of empty and partial capsids in gene therapy products can compromise efficacy, potentially leading to a reduced number of full capsids with therapeutic load, reduced drug efficacy, the need for increased dosing, and an elevated risk of immunogenic responses. The demand for a reliable analytical method for characterizing capsid contents in gene therapy products is increasing in both industry and regulatory spheres as gene therapy gains popularity. Although standard methods such as AUC, CDMS, and Cryo-EM can report F/P/E ratios, they face limitations in throughput, turnaround time, and require further validation. While the AEX analytical technique is favorable for GMP QC environments, it exhibits limitation with baseline separation, making it challenging to distinguish partial capsids from full and empty capsids. In response, we present a novel continuous N-Rich chromatography

approach utilizing two AEX columns for the recycling of a mixed portion containing a high prevalence of partial capsids, allowing for better characterization of partial capsids. Both fraction analysis titrated by qPCR and the discrepancies in retention time between full and partial capsids substantiate rationale for the recycling process. The entire process is monitored through FLRs after each column position, and the application of RFs, ascertained for each full and partial capsid relative to empty capsids, markedly amplifies the accuracy of fluorescence-based signal analysis. The successful development of the N-Rich method provides a consistent F/P/E ratio with an RSD < 5 %. Importantly, this ratio aligns with expected values while providing valuable insights into partial capsids, a capability not observed in other comparative techniques tested. Additionally, the method is developed and optimized using NaOAc, replacing the highly toxic TMAC commonly found in various AEX methods. While the N-Rich method demonstrates successful enhancement in separation of partial capsids and determination of comparable F/P/E ratio, its practical application is currently limited due to the necessity for further investigations on comprehensive validation (increased number of cycles), optimization (shortened batch design and reduced turnaround time), and improvement (recycling based on FLR threshold) of the methodology. Nevertheless, this approach offers a meaningful strategy to enhance the resolution of chromatography-based analytical methods, providing valuable information on partial capsids.

### CRedit authorship contribution statement

**Yong Suk Lee:** Writing – original draft, Visualization, Validation, Project administration, Methodology, Investigation, Funding acquisition, Formal analysis, Data curation, Conceptualization. **Jaeweon Lee:** Writing – original draft, Investigation, Formal analysis. **Kun Fang:** Writing – review & editing, Resources, Formal analysis. **Gretchen V. Gee:** Writing – review & editing, Resources, Formal analysis. **Benjamin Rogers:** Writing – review & editing, Resources, Formal analysis. **David McNally:** Writing – review & editing, Resources, Formal analysis, Conceptualization. **Seongkyu Yoon:** Writing – review & editing, Supervision, Resources, Project administration, Methodology, Investigation, Funding acquisition, Conceptualization.

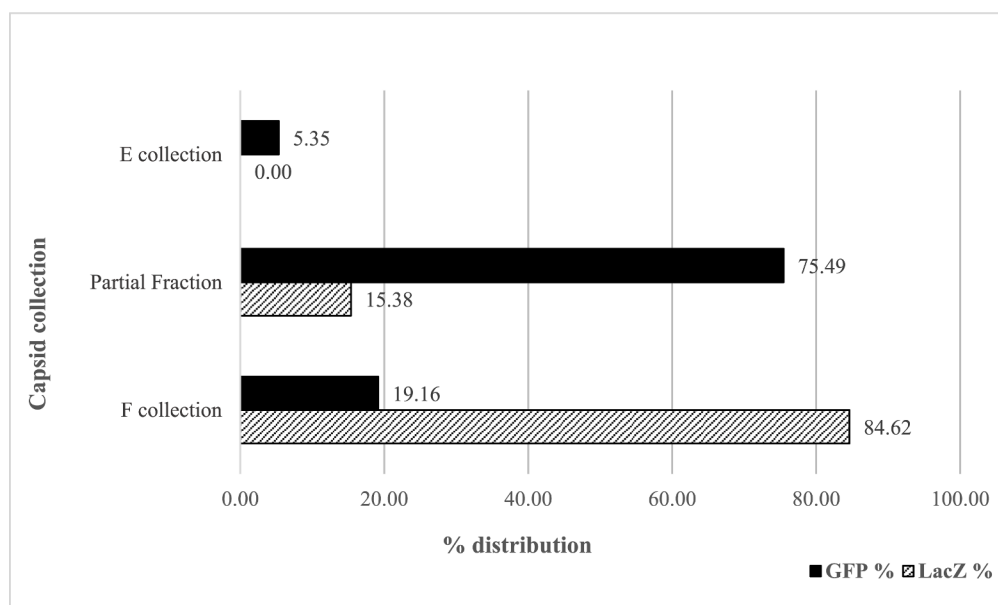


**Fig. 8. Capsid distribution and purity check across separated samples.** Purity of separated capsid collections were assessed by qPCR assays. F and E capsids were collected via designated separate outlets during the N-Rich process. P capsids were collected via fraction collector during the final elution step of N-Rich. The separation and distribution of P capsids were assessed by qPCR using primer/probe specific for GFP gene, and F capsids were assessed using qPCR assay targeting LacZ gene.

## Declaration of competing interest

The authors declare that they have no known competing financial interests or personal relationships that could have appeared to influence the work reported in this paper.

## Data availability

Data will be made available on request.

## Acknowledgments

- This work was performed under a Project Award Agreement from the National Institute for Innovation in Manufacturing Biopharmaceuticals (NIIMBL) and financial assistance award 70NANB17H002 from the U.S. Department of Commerce, National Institute of Standards and Technology (NIST).
- The authors thank George Liang, Qiang Fu, and Yongdan Wang at University of Massachusetts Lowell, United States, for their assistance with the experiments and their insightful comments.
- The authors thank Electron Microscopy Core Facility at UMass Chan Medical School, United States, especially Dr. Kyoungwan Lee, for his assistance with TEM imaging and analysis.
- The authors acknowledge YMC ChromaCon, United States, particularly Richard Weldon and Sebastian Vogg, for their assistance and consultations with Contichrom Cube system.

## Appendix A. Supplementary material

Supplementary data to this article can be found online at <https://doi.org/10.1016/j.jchromb.2024.124206>.

## References

- P.D. Robbins, H. Tahara, S.C. Ghivizzani, Viral vectors for gene therapy, *Trends Biotechnol.* 16 (1) (1998) 35–40.
- X. Pan, et al., Applications and developments of gene therapy drug delivery systems for genetic diseases, *Asian J. Pharm. Sci.* 16 (6) (2021) 687–703.
- T. Athanasopoulos, S. Fabb, G. Dickson, Gene therapy vectors based on adeno-associated virus: characteristics and applications to acquired and inherited diseases (review), *Int. J. Mol. Med.* 6 (4) (2000) 363–375.
- M.F. Naso, et al., Adeno-Associated Virus (AAV) as a Vector for Gene Therapy, *BioDrugs* 31 (4) (2017) 317–334.
- A. Patel, et al., Design of AAV vectors for delivery of large or multiple transgenes, *Methods Mol. Biol.* 1950 (2019) 19–33.
- D.A. Kuzmin, et al., The clinical landscape for AAV gene therapies, *Nat. Rev. Drug Discov.* 20 (3) (2021) 173–174.
- J. Gao, R.M. Hussain, C.Y. Weng, Voretigene neparvovec in retinal diseases: a review of the current clinical evidence, *Clin. Ophthalmol.* 14 (2020) 3855–3869.
- T. Ogbonmide, et al., Gene Therapy for Spinal Muscular Atrophy (SMA): a review of current challenges and safety considerations for Onasemnogene Apeparvovec (Zolgensma), *Cureus* 15 (3) (2023) e36197.
- J.A. Tice, et al., The effectiveness and value of gene therapy for hemophilia: A Summary from the Institute for Clinical and Economic Review's California Technology Assessment Forum, *J. Manag. Care Spec. Pharm.* 29 (5) (2023) 576–581.
- H.A. Blair, Valoctocogene roxaparvovec: first approval, *Drugs* 82 (14) (2022) 1505–1510.
- S.J. Keam, Epladocogene exuparvovec: first approval, *Drugs* 82 (13) (2022) 1427–1432.
- Y. Wang, et al., Decoding cellular mechanism of recombinant adeno-associated virus (rAAV) and engineering host-cell factories toward intensified viral vector manufacturing, *Biotechnol. Adv.* 71 (2024) 108322.
- Q. Fu, et al., Critical challenges and advances in recombinant adeno-associated virus (rAAV) biomanufacturing, *Biotechnol. Bioeng.* 120 (9) (2023) 2601–2621.
- A.F. Meier, C. Fraefel, M. Seyffert, The interplay between adeno-associated virus and its helper viruses, *Viruses* 12 (6) (2020).
- G. Chadeuf, et al., Evidence for encapsidation of prokaryotic sequences during recombinant adeno-associated virus production and their in vivo persistence after vector delivery, *Mol. Ther.* 12 (4) (2005) 744–753.
- M. Schnödt, H. Büning, Improving the quality of adeno-associated viral vector preparations: the challenge of product-related impurities, *Hum. Gene Ther. Methods* 28 (3) (2017) 101–108.
- Q. Fu, et al., Design space determination to optimize DNA complexation and full capsid formation in transient rAAV manufacturing, *Biotechnol. Bioeng.* 120 (11) (2023) 3148–3162.
- T.N.T. Nguyen, et al., Mechanistic model for production of recombinant adeno-associated virus via triple transfection of HEK293 cells, *Mol. Ther. Methods Clin. Dev.* 21 (2021) 642–655.
- T. Weber, Anti-AAV Antibodies in AAV gene therapy: current challenges and possible solutions, *Front. Immunol.* 12 (2021) 658399.
- K. Gao, et al., Empty Virions In AAV8 vector preparations reduce transduction efficiency and may cause total viral particle dose-limiting side-effects, *Mol. Ther. Methods Clin. Dev.* 1 (9) (2014) 20139.
- G. Qu, et al., Separation of adeno-associated virus type 2 empty particles from genome containing vectors by anion-exchange column chromatography, *J. Virol. Methods* 140 (1–2) (2007) 183–192.
- M. Hösel, et al., Toll-like receptor 2-mediated innate immune response in human nonparenchymal liver cells toward adeno-associated viral vectors, *Hepatology* 55 (1) (2012) 287–297.
- F. Mingozzi, et al., CD8(+) T-cell responses to adeno-associated virus capsid in humans, *Nat. Med.* 13 (4) (2007) 419–422.
- V. Louis Jeune, et al., Pre-existing anti-adeno-associated virus antibodies as a challenge in AAV gene therapy, *Hum. Gene Ther. Methods* 24 (2) (2013) 59–67.
- Y. Wang, et al., Transcriptomic features reveal molecular signatures associated with recombinant adeno-associated virus production in HEK293 cells, *Biotechnol. Prog.* 39 (4) (2023) e3346.
- J.F. Wright, Product-related impurities in clinical-grade recombinant AAV vectors: characterization and risk assessment, *Biomedicines* 2 (1) (2014) 80–97.
- J.F. Wright, Quality control testing, characterization and critical quality attributes of adeno-associated virus vectors used for human gene therapy, *Biotechnol. J.* 16 (1) (2021) 2000022.
- T.R. Flotte, Empty adeno-associated virus capsids: contaminant or natural decoy? *Hum. Gene Ther.* 28 (2) (2017) 147–148.
- R. Rieser, et al., Comparison of different liquid chromatography-based purification strategies for adeno-associated virus vectors, *Pharmaceutics* 13 (5) (2021).
- R.J. Samulski, N. Muzyczka, AAV-mediated gene therapy for research and therapeutic purposes, *Annu. Rev. Virol.* 1 (1) (2014) 427–451.
- B. Leuchs, et al., A novel scalable, robust downstream process for oncolytic rat parvovirus: isoelectric point-based elimination of empty particles, *Appl. Microbiol. Biotechnol.* 101 (8) (2017) 3143–3152.
- S. Subramanian, et al., Filling adeno-associated virus capsids: estimating success by cryo-electron microscopy, *Hum. Gene Ther.* 30 (12) (2019) 1449–1460.
- X. Fu, et al., Analytical strategies for quantification of adeno-associated virus empty capsids to support process development, *Hum. Gene Ther. Methods* 30 (4) (2019) 144–152.
- A.K. Werle, et al., Comparison of analytical techniques to quantitate the capsid content of adeno-associated viral vectors, *Mol. Ther. Methods Clin. Dev.* 23 (2021) 254–262.
- N.L. McIntosh, et al., Comprehensive characterization and quantification of adeno associated vectors by size exclusion chromatography and multi angle light scattering, *Sci. Rep.* 11 (1) (2021) 3012.
- J.M. Sommer, et al., Quantification of adeno-associated virus particles and empty capsids by optical density measurement, *Mol. Ther.* 7 (1) (2003) 122–128.
- E.E. Pierson, et al., Resolving adeno-associated viral particle diversity with charge detection mass spectrometry, *Anal. Chem.* 88 (13) (2016) 6718–6725.
- A.L. Gimpel, et al., Analytical methods for process and product characterization of recombinant adeno-associated virus-based gene therapies, *Mol. Ther. Methods Clin. Dev.* 20 (2021) 740–754.
- Z. Wu, et al., Development of a two-dimensional liquid chromatography-mass spectrometry platform for simultaneous multi-attribute characterization of adeno-associated viruses, *Anal. Chem.* 94 (7) (2022) 3219–3226.
- S.L. Khatwani, A. Pavlova, Z. Pirot, Anion-exchange HPLC assay for separation and quantification of empty and full capsids in multiple adeno-associated virus serotypes, *Mol. Ther. Methods Clin. Dev.* 21 (2021) 548–558.
- E. Ayuso, F. Mingozzi, F. Bosch, Production, purification and characterization of adeno-associated vectors, *Curr. Gene Ther.* 10 (6) (2010) 423–436.
- S. Zolotukhin, et al., Production and purification of serotype 1, 2, and 5 recombinant adeno-associated viral vectors, *Methods* 28 (2) (2002) 158–167.
- C. Wang, et al., Developing an Anion Exchange Chromatography Assay for Determining Empty and Full Capsid Contents in AAV6.2, *Mol. Ther. Methods Clin. Dev.* 15 (2019) 257–263.
- N. Kaludov, B. Handelman, J.A. Chiorini, Scalable purification of adeno-associated virus type 2, 4, or 5 using ion-exchange chromatography, *Hum Gene Ther* 13 (10) (2002) 1235–1243.
- A. Lošdorfer Božič, A. Siber, R. Podgornik, How simple can a model of an empty viral capsid be? Charge distributions in viral capsids, *J Biol Phys* 38 (4) (2012) 657–671.
- C.L. Heldt, et al., Empty and Full AAV Capsid Charge and Hydrophobicity Differences Measured with Single-Particle AFM, *Langmuir* 39 (16) (2023) 5641–5648.
- R. Dickerson, et al., Separating Empty and Full Recombinant Adeno-Associated Virus Particles Using Isoelectric Anion Exchange Chromatography, *Biotechnol J* 16 (1) (2021) e2000015.
- P. Gagnon, et al., Multiple-Monitor HPLC Assays for Rapid Process Development, In-Process Monitoring, and Validation of AAV Production and Purification, *Pharmaceutics* 13 (1) (2021).

- [49] A.E. Yarawsky, et al., AAV analysis by sedimentation velocity analytical ultracentrifugation: beyond empty and full capsids, *Eur Biophys J* 52 (4–5) (2023) 353–366.
- [50] M.K. Aebischer, et al., Anion-exchange chromatography at the service of gene therapy: baseline separation of full/empty adeno-associated virus capsids by screening of conditions and step gradient elution mode, *Int. J. Mol. Sci.* 23 (20) (2022).
- [51] R. Weldon, T. Müller-Späth, Enrichment and purification of peptide impurities using twin-column continuous chromatography, *J Chromatogr A* 1667 (2022) 462894.
- [52] G. Lievore, et al., Enrichment and recovery of oligonucleotide impurities by N-Rich twin-column continuous chromatography, *J Chromatogr B Analyt Technol Biomed Life Sci* 1209 (2022) 123439.
- [53] E. Bigelow, et al., Using continuous chromatography methodology to achieve high-productivity and high-purity enrichment of charge variants for analytical characterization, *J Chromatogr A* 1643 (2021) 462008.
- [54] S.Y. Jing, et al., A novel twin-column continuous chromatography approach for separation and enrichment of monoclonal antibody charge variants, *Eng Life Sci* 21 (6) (2021) 382–391.
- [55] T.K. Kim, et al., Experimental Design of the Multicolumn Countercurrent Solvent Gradient Purification (MCSGP) Unit for the Separation of PEGylated Proteins, *Ind. Eng. Chem. Res.* 60 (29) (2021) 10764–10776.
- [56] M. Florea, et al., High-efficiency purification of divergent AAV serotypes using AAVX affinity chromatography, *Mol Ther Methods Clin Dev* 28 (2023) 146–159.
- [57] O. Khanal, V. Kumar, M. Jin, Adeno-associated viral capsid stability on anion exchange chromatography column and its impact on empty and full capsid separation, *Mol Ther Methods Clin Dev* 31 (2023) 101112.
- [58] H. Yang, S. Koza, W. Chen, Waters-an anion-exchange chromatography method for monitoring empty capsid content in adeno-associated virus serotype AAV8, *Appl. Notebook* 38 (6) (2020) 369–370.
- [59] C. Lu, et al., Using the intrinsic fluorescence of DNA to characterize aptamer binding, *Molecules* 27 (22) (2022) 7809.